PROCEEDINGS of the
23rd International Congress on Acoustics

9 to 13 September 2019 in Aachen, Germany

Theoretical model for the prediction of sound radiated from unbaffled long enclosure with ground effect

Weiping YANG[1]; Yatsze CHOY[2]

[1, 2] The Hong Kong Polytechnic University, Hong Kong, P. R. China

ABSTRACT

A theoretical model is presented for the prediction of sound radiated from an unbaffled long enclosure with ground effect. This geometrical arrangement forms an idealized representation of traffic facilities such as tunnels and railway stations where sound propagates along the enclosures and radiates to the outside through the openings at both ends. The sound fields inside and outside the enclosures should be accurately predicted and thoroughly analyzed so as to determine an appropriate noise control strategy. In this paper, the Fourier transform technique and the mode matching method are firstly applied to transform the intractable boundary value problem into a scalar modified Wiener-Hopf equation. The solution of which contains infinitely many unknowns satisfying infinite linear algebraic equations susceptible to numerical treatment. Good agreement is found between the solutions obtained by the finite element method (FEM) and the proposed technique in a wide frequency range. Then, the far-field directivity patterns of the outside acoustic fields are emphatically illustrated and the formation mechanisms of lobes, zeros and the after radiation are discussed in details. In the end, the advantages and the application prospects of the proposed method are summarized.

Keywords: Sound radiation, Unbaffled long enclosure, Wiener-Hopf technique

1. INTRODUCTION

In order to predict and control the noise level inside tunnels and railway stations, much attention has been focused in recent years on the mechanisms of sound propagation and dissipation inside long enclosures (1). Hard rough surfaces (2) and sound-absorbing materials (3) are found to be effective in reducing this kind of noise. However, in literatures, the enclosures were usually assumed to be infinite long and only the sound field deep inside the enclosures were considered. Reflection waves due to the abrupt size change of the openings were ignored which should be taken into consideration in practical applications as they contribute significantly to the total sound field especially near the opening.

As the noise is difficult to be transmitted outside through the wall, it will concentrate at both ends of the long enclosures and radiate to the outside through the portals. If there are residents nearby, their living conditions will be severely deteriorated. Under such circumstance, the pollution caused by the radiated sound become prominent. When the prediction of sound level radiated from long enclosures is required, recourses are often made to simplify the geometry in which the openings are imagined to be surrounded by infinite baffle, thereby eliminating the diffraction effect of edge. In this condition, the Rayleigh integral (4) can be applied. However, it is only available to calculate the sound field in front of the opening while the radiation to the back side which is heavily influenced by the edge diffraction cannot be predicted. Besides, the model assumes that the outside region is free field, while in practical tunnels, the ground cannot be ignored which divides the total acoustic domain into a semi-infinite one and makes the problem more complicated.

The main difference between the problem at hand and that in the literatures is that the unbaffled opening of the long enclosure and the ground effect are taken into account simultaneously in order to model the real traffic facilities. However, due to the geometrical complexity, this boundary value problem cannot be solved analytically for the lack of known conditions in the natural domain. During the past decades, several attempts were done by researchers to find the solution of the problem from different perspectives. In 1998, the Research Committee of Road Traffic Noise in Acoustic Society of

[1] w.p.yang@connect.polyu.hk
[2] yatsze.choy@polyu.edu.hk

Japan established the ASJ model (5) to predict the sound radiated from tunnel opening based on the principal of energy conservation. However, it can only be applied as an approximate approach for engineering applications as the correction terms for the edge diffraction and the ground effect in the model are either from experimental data or empirical formula (6). In addition, numerical methods based on the FEM (7, 8) were proposed to transform the semi-infinite acoustic domain outside the enclosure into a waveguide one by introducing a perfectly matched layer (PML) outside the original geometry. Then, the radiated sound field can be easily obtained through the traditional mode matching method. However, their computational efficiency are limited by the size of the geometry which limits their application in dealing with problems regarding traffic noise.

Wiener-Hopf technique is fairly a standard method to solve certain type of linear partial differential equations subjected to mixed boundary conditions on semi-infinite geometries. The exact solution to the problem of plane wave radiation from a cylindrical duct to the free field was obtained using the method by H. Levine (9). Then, it was extensively applied to solve problems regarding sound radiation from waveguide (10). Based on the existing literatures, we try to extend its application to obtain the explicit solution of the sound fields inside and outside a semi-infinite long enclosure. In the model, the unbaffled opening as well as the ground effect will be considered simultaneously which are seldom addressed before. In addition, the accuracy and efficiency of the proposed method will be compared with the FEM to highlight its availability and advantages in predicting traffic noise.

2. FORMULATION

2.1 Boundary Value Problem

Consider a two-dimensional semi-infinite long enclosure as shown in Figure 1. The thickness of the wall is zero and all the surfaces are assumed to be acoustical rigid for simplicity. The origin of the coordinate system is at the intersection of the opening and the ground. Imaginary interfaces I and II are depicted for analysis convenience. They divide the total sound field into three sub-regions A, B and C which will be analyzed separately later.

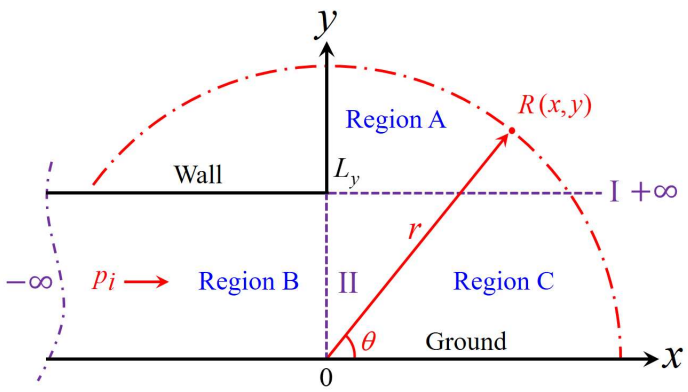

Figure 1 – Schematic diagram of sound radiation from unbaffled long enclosure with ground

The total sound pressure field can be expressed by the following piecewise function

$$p_T(x,y)=\begin{cases} p_A(x,y) & x\in(-\infty,+\infty)\cap y\in\left[L_y,+\infty\right) \\ p_i(x,y)+p_B(x,y) & x\in(-\infty,0]\cap y\in\left[0,L_y\right] \\ p_C(x,y) & x\in[0,+\infty)\cap y\in\left[0,L_y\right] \end{cases} \tag{1}$$

where L_y denotes the height of the outer wall. $p_A(x,y)$, $p_B(x,y)$ and $p_C(x,y)$ stand for the scattered sound fields in sub-regions A, B and C, respectively. Assume that a plane acoustic wave is incident from the left-hand side of the long enclosure which is given by

$$p_i(x,y)=e^{-ikx} \tag{2}$$

where k denotes the free space wave number. The time dependent factor $e^{i\omega t}$ with ω being the angular frequency is well known and will be suppressed throughout. Noted that in any physical medium, loss is inevitable. Therefore, the ideal lossless medium which is often used in theoretical analysis, can be

regarded as the limiting case with vanishingly small loss. It is convenient to retain a small but nonzero loss in the model for further study, namely, let

$$k = k_1 - ik_2, \quad k_1 \gg k_2 > 0 \tag{3}$$

So, the purely lossless medium is considered as the limiting case when k_2 tends to be zero. The total sound field satisfies the Helmholtz equation

$$\nabla^2 p_T(x,y) + k^2 p_T(x,y) = 0 \tag{4}$$

where ∇^2 denotes the two-dimensional Laplace operator. The total sound field is to be determined by the boundary conditions at the surfaces

$$\partial p_A(x,L_y)/\partial y = 0, \quad x \in (-\infty, 0] \tag{5}$$

$$\partial p_B(x,L_y)/\partial y = 0, \quad x \in (-\infty, 0] \tag{6}$$

$$\partial p_B(x,0)/\partial y = 0, \quad x \in (-\infty, 0] \tag{7}$$

$$\partial p_C(x,0)/\partial y = 0, \quad x \in [0, +\infty) \tag{8}$$

the continuity relations at the imaginary interface I

$$p_A(x,L_y) = p_C(x,L_y), \quad x \in [0, +\infty) \tag{9}$$

$$\partial p_A(x,L_y)/\partial y = \partial p_C(x,L_y)/\partial y, \quad x \in [0, +\infty) \tag{10}$$

and the continuity relations at the imaginary interface II

$$p_i(0,y) + p_B(0,y) = p_C(0,y), \quad y \in [0, L_y] \tag{11}$$

$$\partial[p_i(0,y) + p_B(0,y)]/\partial x = \partial p_C(0,y)/\partial x, \quad y \in [0, L_y] \tag{12}$$

The acoustic field of interest involves boundaries at infinity and geometrical singularity at the edge which may give rise to several mathematically acceptable solutions of the Helmholtz equation. Only one of them, however, is consistent with the anticipated physical phenomenon. In order to ensure the uniqueness of the solution, the Sommerfeld radiation condition at infinity

$$\lim_{r\to\infty} \sqrt{r}\left[\partial p_T(r,\theta)/\partial r - ikp_T(r,\theta)\right] = 0, \quad r = \sqrt{x^2 + y^2} \tag{13}$$

should be satisfied. Besides, according to the edge condition, the acoustic energy stored in any finite neighborhood of the edge must be finite (11).

Up to now, the boundary value problem has been well described in the natural domain. Due to the existence of semi-infinite region, however, the solution cannot be directly obtained. The Wiener-Hopf technique in conjunction with the mode matching method will be applied to transform the intractable problem into the spectral domain and obtain the Wiener- Hopf equation which can be solved through analytic continuation procedures. Essentially, this mixed method depends on expanding the sound field inside the enclosure by normal modes and applying the Fourier transform technique elsewhere which permits us to obtain the solution by the continuous relations at the opening.

2.2 Wiener-Hopf Equation and Its Solution

When applying the Wiener-Hopf technique, the Fourier integral and its inverse transformation are required which are defined as follows

$$F(\alpha,y) = \int_{-\infty}^{+\infty} f(x,y) e^{-i\alpha x} dx, \quad f(x,y) = \frac{1}{2\pi} \int_{-\infty}^{+\infty} F(\alpha,y) e^{i\alpha x} d\alpha \tag{14}$$

where $f(x,y)$ stands for arbitrary function in the natural domain and $F(\alpha,y)$ denotes the corresponding transformed function in the spectral domain. In Eq.(14), the complex parameter $\alpha = \sigma + i\tau$ is the Fourier transform variable. Since $p_A(x,y)$ satisfies the Helmholtz equation, its Fourier transform with respect to x gives

$$\partial^2 P_A(\alpha,y)/\partial y^2 + K^2(\alpha) P_A(\alpha,y) = 0 \tag{15}$$

where $K(\alpha) = \sqrt{k^2 - \alpha^2}$. The sound pressure of region A in the spectral domain can be divided into two parts based on the definition of half range Fourier transform as

$$P_A(\alpha,y) = P_A^-(\alpha,y) + P_A^+(\alpha,y) = \int_{-\infty}^{0} p_A(x,y) e^{-i\alpha x} dx + \int_{0}^{+\infty} p_A(x,y) e^{-i\alpha x} dx \tag{16}$$

The plus and minus signs in the superscript of the transformed function indicate that they are analytic

functions in upper and lower half complex plane, respectively. By taking into account the following asymptotic behavior of outgoing wave at infinity

$$p_A(x,y) = O\left(e^{-ik|x|}\right), \quad x \to \pm\infty \tag{17}$$

one can show that $P_A^+(\alpha, y)$ and $P_A^-(\alpha, y)$ are regular functions in the upper half complex plane defined by $\tau > -k_2$ and the lower half complex plane defined by $\tau < k_2$, respectively. The general solution of Eq.(15) satisfying the radiation condition in the spectral domain reads

$$P_A(\alpha, y) = A(\alpha) e^{-iK(\alpha)(y - L_y)} \tag{18}$$

where $A(\alpha)$ is an unknown coefficient to be determined. Obviously, the square root function $K(\alpha)$ is double-valued in the complex plane. Therefore, it is necessary to specify its branches so as to uniquely define it. As shown in Figure 2, for the function $K(\alpha)$, there are two branch points $\pm k$ and two branch cuts along $\alpha = +k$ to $\alpha = +k - i\infty$ and $\alpha = -k$ to $\alpha = -k + i\infty$, so that $K(0) = k$.

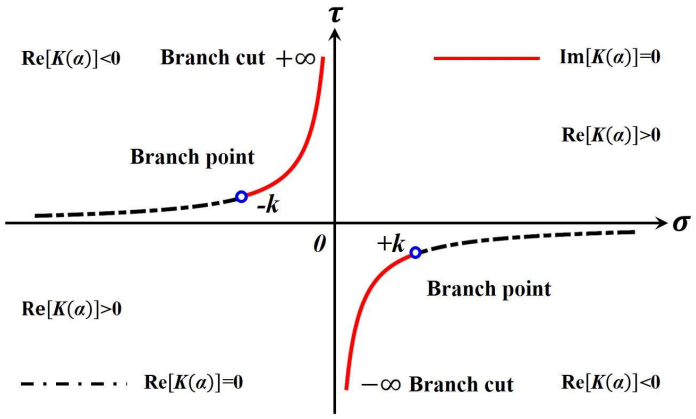

Figure 2 – Branch cuts of the square root function in the complex plane

Using the derivative of Eq.(18) with respect to y and the transformed form of Eq.(5) we have

$$\dot{P}_A^+(\alpha, L_y) = -iK(\alpha) A(\alpha) \tag{19}$$

where the dot specifies the derivative with respect to y. Similarly, we convert the Helmholtz equation for region C into the spectral domain by using the half-range Fourier transform technique

$$\partial^2 P_C^+(\alpha, y)/\partial y^2 + K^2(\alpha) P_C^+(\alpha, y) = f(y) + i\alpha g(y) \tag{20}$$

where the new functions in Eq.(20) are defined as

$$f(y) = \partial p_C(0, y)/\partial x, \quad g(y) = p_C(0, y) \tag{21}$$

The general solution of Eq.(20) can be attained by using the method of constant variation

$$P_C^+(\alpha, y) = B(\alpha)\cos\left[K(\alpha) y\right] + C(\alpha)\sin\left[K(\alpha) y\right] + \frac{1}{K(\alpha)} \int_0^y \left[f(t) + i\alpha g(t)\right] \sin\left[K(\alpha)(y - t)\right] dt \tag{22}$$

where $B(\alpha)$ and $C(\alpha)$ are unknown coefficients. Using the transformed form of Eq.(8), the coefficients can be determined. Then, the sound field of region C in the spectral domain reads

$$\begin{aligned} P_C^+(\alpha, y) = &-\frac{\cos\left[K(\alpha) y\right]}{K(\alpha)\sin\left[K(\alpha) L_y\right]} \left\{ \dot{P}_A^+(\alpha, L_y) - \int_0^{L_y} \left[f(t) + i\alpha g(t)\right] \cos\left[K(\alpha)\left(L_y - t\right)\right] dt \right\} \\ &+ \frac{1}{K(\alpha)} \int_0^y \left[f(t) + i\alpha g(t)\right] \sin\left[K(\alpha)(y - t)\right] dt \end{aligned} \tag{23}$$

Noted that the left-hand side of Eq.(23) is regular in the upper half complex plane. However, the regularity of the right-hand side of the equation is violated by the presence of simple poles occurring at the zeros of denominator, namely, $\alpha = \alpha_m$ satisfying

$$K(\alpha_m)\sin\left[K(\alpha_m) L_y\right] = 0, \quad \mathrm{Im}(\alpha_m) < \mathrm{Im}(k), \quad m = 0, 1, 2, \ldots \tag{24}$$

These poles can be eliminated by imposing that their residues are zero. This gives

$$\dot{P}_A^+\left(\alpha_m, L_y\right) = Q_m\left(f_m + i\alpha_m g_m\right)(-1)^m \tag{25}$$

where the coefficients f_m and g_m are defined as

$$\begin{bmatrix} f_m \\ g_m \end{bmatrix} = \frac{1}{Q_m}\int_0^{L_y}\begin{bmatrix} f(t) \\ g(t) \end{bmatrix}\cos\left[K\left(\alpha_m\right)t\right]dt \tag{26}$$

The coefficient Q_m is the norm of these series expansion which is defined as

$$Q_m = \int_0^{L_y}\cos^2\left[K\left(\alpha_m\right)t\right]dt = \frac{L_y}{2}(1+\delta_{0\mathrm{m}}) \tag{27}$$

where δ denotes the delta function. Consider now the transformed pressure continuity at the imaginary interface I and using Eq. (16) and Eq.(23) we have

$$\frac{\dot{P}_A^+\left(\alpha, L_y\right)}{K^2(\alpha)L(\alpha)} - P_A^-\left(\alpha, L_y\right) = \frac{1}{K(\alpha)\sin\left[K(\alpha)L_y\right]}\int_0^{L_y}\left[f(t)+i\alpha g(t)\right]\cos\left[K(\alpha)t\right]dt \tag{28}$$

where the kernel function is expressed as

$$L(\alpha) = \frac{\sin\left[K(\alpha)L_y\right]}{K(\alpha)}e^{-iK(\alpha)L_y} \tag{29}$$

Owing to Eq.(26) the defined functions can be expanded into cosine series as follows

$$\begin{bmatrix} f(t) \\ g(t) \end{bmatrix} = \sum_{m=0}^{\infty}\begin{bmatrix} f_m \\ g_m \end{bmatrix}\cos\left[K\left(\alpha_m\right)t\right] \tag{30}$$

Substituting Eq.(30) into Eq.(28) and evaluating the resultant integral, one obtains the scalar modified Wiener-Hopf equation of the second kind which is valid in the strip $-k_2 < \tau < k_2$ as

$$\frac{\dot{P}_A^+\left(\alpha, L_y\right)}{K^2(\alpha)L(\alpha)} - P_A^-\left(\alpha, L_y\right) = -\sum_{m=0}^{\infty}\left(f_m + i\alpha g_m\right)\frac{(-1)^m}{\alpha^2-\alpha_m^2} \tag{31}$$

The solution of Eq.(31) can be obtained through the classical Wiener-Hopf procedure (12) as

$$\dot{P}_A^+\left(\alpha, L_y\right) = \sum_{m=0}^{\infty}(-1)^m\frac{f_m - i\alpha_m g_m}{2\alpha_m\left(\alpha+\alpha_m\right)}\left(k+\alpha_m\right)L^+\left(\alpha_m\right)\left(k+\alpha\right)L^+\left(\alpha\right) \tag{32}$$

Here the split function is regular and free of zeros in the upper half plane which is given by

$$\begin{aligned} L^+(\alpha) = {} & \sqrt{\frac{\sin\left(kL_y\right)}{k}}\times\exp\left\{\ln\left[\frac{\alpha - iK(\alpha)}{k}\right]\frac{K(\alpha)L_y}{\pi}\right\} \\ & \times\exp\left\{\left(1-C+\ln\left(\frac{2\pi}{kL_y}\right)-\frac{i\pi}{2}\right)\frac{-i\alpha L_y}{\pi}\right\}\times\prod_{m=1}^{\infty}\left(1+\frac{\alpha}{\alpha_m}\right)\times\exp\left(\frac{-i\alpha L_y}{m\pi}\right) \end{aligned} \tag{33}$$

where C is the Euler's constant given by $C = 0.57721\ldots$

2.3 Determination of the Sound Fields

As can be seen, Eq.(32) contains infinite number of unknown coefficients. To determine them, the well-known mode matching method will be applied. The scattered sound field in region B can be expressed in terms of normal modes as

$$p_B(x,y) = \sum_{n=0}^{\infty}a_n\cos\left[K\left(\alpha_n\right)y\right]e^{i\alpha_n x} \tag{34}$$

where the eigenvalues are evaluated by the boundary conditions as

$$K\left(\alpha_n\right) = \frac{n\pi}{L_y},\quad \alpha_n = \sqrt{k^2-\left(\frac{n\pi}{L_y}\right)^2},\ n = 0,1,2,\ldots \tag{35}$$

Based on the continuity relations at the opening, we have the following identities

$$\sum_{m=0}^{\infty}f_m\cos\left[K\left(\alpha_m\right)y\right] = -ik + i\sum_{n=0}^{\infty}a_n\alpha_n\cos\left[K\left(\alpha_n\right)y\right] \tag{36}$$

$$\sum_{m=0}^{\infty}g_m\cos\left[K\left(\alpha_m\right)y\right] = 1+\sum_{n=0}^{\infty}a_n\cos\left[K\left(\alpha_n\right)y\right] \tag{37}$$

Multiply both sides of the equations by $\cos\left[K(\alpha_s)y\right]$ and integrate from zero to L_y in terms of y, using the orthogonality of the modal functions, we have

$$f_0 = -ik(1-a_0),\ s=0, \quad f_s = i\alpha_s a_s,\ s\neq 0 \tag{38}$$

$$g_0 = 1+a_0,\ s=0, \quad g_s = a_s,\ s\neq 0 \tag{39}$$

On the other hand, combine Eq.(25) and Eq.(32) together when a new index s is used, we have

$$Q_s\left(f_s + i\alpha_s g_s\right)(-1)^s = \sum_{m=0}^{\infty}(-1)^m \frac{f_m - i\alpha_m g_m}{2\alpha_m(\alpha_s+\alpha_m)}(k+\alpha_m)L^+(\alpha_m)(k+\alpha_s)L^+(\alpha_s) \tag{40}$$

Substitute Eq.(38) and Eq.(39) into Eq.(40) we have the following identity

$$a_s = (-1)^{s+1}\frac{k}{Q_s\alpha_s}L^+(k)L^+(\alpha_s) \tag{41}$$

which are the modal coefficients of region B. Then, by Eq.(34) the sound field inside the enclosure can be determined. The radiated sound field in region A can be obtained by taking the inverse Fourier transform of $P_A(\alpha,y)$ as

$$p_A(x,y) = \frac{1}{2\pi}\int_{\Gamma}\frac{\dot{P}_A^+(\alpha,L_y)}{-iK(\alpha)}e^{-iK(\alpha)(y-L_y)}e^{i\alpha x}d\alpha \tag{42}$$

where Γ is a straight line parallel to the real axis lying in the strip $-k_2 < \tau < k_2$. In order to perform the asymptotic evaluation of the equation via the saddle point technique, let us change the variables and express the radiated sound field in cylindrical polar coordinate system as shown in Figure 1.

$$\alpha = -k\cos w, \quad x = r\cos\theta, \quad y = r\sin\theta \tag{43}$$

Then, the radiated field can be determined (12) as

$$p_A(r,\theta) = \frac{e^{i\pi/4}}{\sqrt{2\pi}}2kL^+(-k\cos\theta)L^+(k)e^{ik\sin\theta L_y}\frac{e^{-ikr}}{\sqrt{kr}} \tag{44}$$

Up to now, the sound fields inside and outside the semi-infinite long enclosure are obtained. Next, the FEM will be applied to validate the proposed model.

3. DISCUSSIONS

An enclosure of 2.5m long and 0.5m high is established in COMSOL Multiphysics, a commercial software based on the finite element method (FEM), to validate the proposed technique. In theory, the radiated sound field extends to infinity. However, for the computational efficiency, a relatively small calculation domain is considered. The outside acoustic domain is bounded by introducing PML which is an artificial absorbing layer allowing sound wave to propagate out without reflection. The results of absolute sound pressure in region B at 800Hz obtained by the Wiener-Hopf technique and the FEM are compared in Figure 3.

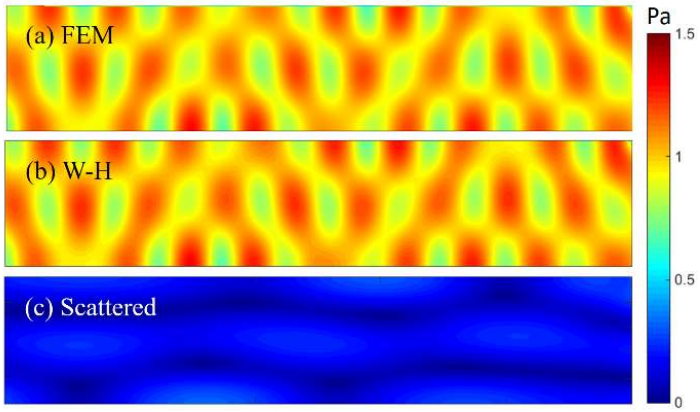

Figure 3 – Comparison of the sound fields in region B (absolute sound pressure/ Pa) obtained by Wiener-Hopf technique (W-H) and the FEM at 800Hz

From (a) and (b) we can observe good agreement between the results obtained by the Wiener-Hopf

technique and the FEM. From (c), we can find that, inside the enclosure, apart from the incident plane wave, the scattered wave will contribute to the total sound field due to the impedance mismatch at the opening. For small size enclosure with plane wave incidence in this case, the scatted field is relatively small and simply distributed. But it cannot be ignored as it still contributes nearly 1/3 of the sound energy. For larger size enclosure and in high frequency case, the contribution will increase.

Besides, comparison of sound pressure level (dB) between the Wiener-Hopf technique and the FEM in the frequency range 200Hz to 2000Hz at a particular point (-0.1,0.35) near the opening edge is also shown in Figure 4. In this case, 100 modes are taken in the calculation. Good agreement is found which validates the correctness and accuracy of the proposed model.

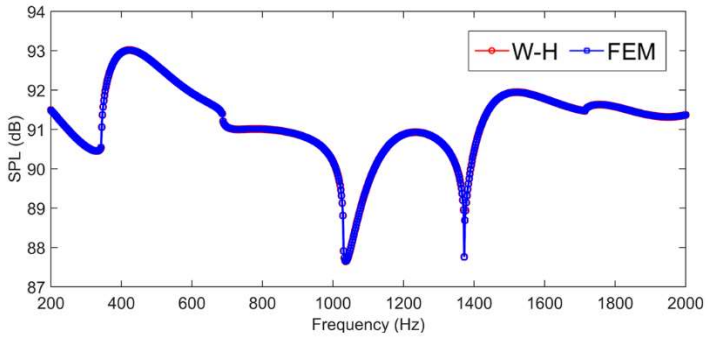

Figure 4 – Comparison of sound pressure level (dB) between Wiener-Hopf technique and FEM in the frequency range 200Hz to 2000Hz at a particular point (-0.1,0.35)

Directivity patterns of the radiated sound field in region A at different frequencies are plotted in polar coordinate (r=5m). As shown in Figure 5, the results show good agreement despite some sharp deeps which may come from mathematical issues. Clear lobes and zeros can be observed. The number of lobes increases with the increasing of frequency. In front of the opening, the sound field is formed by the superposition of radiated, diffracted and reflected sound. They propagate to the receiver with different phase and distance, which results in the directivity pattern. At the back, the sound field is the result of diffraction at the opening edge. It becomes stable and stands at relatively low level.

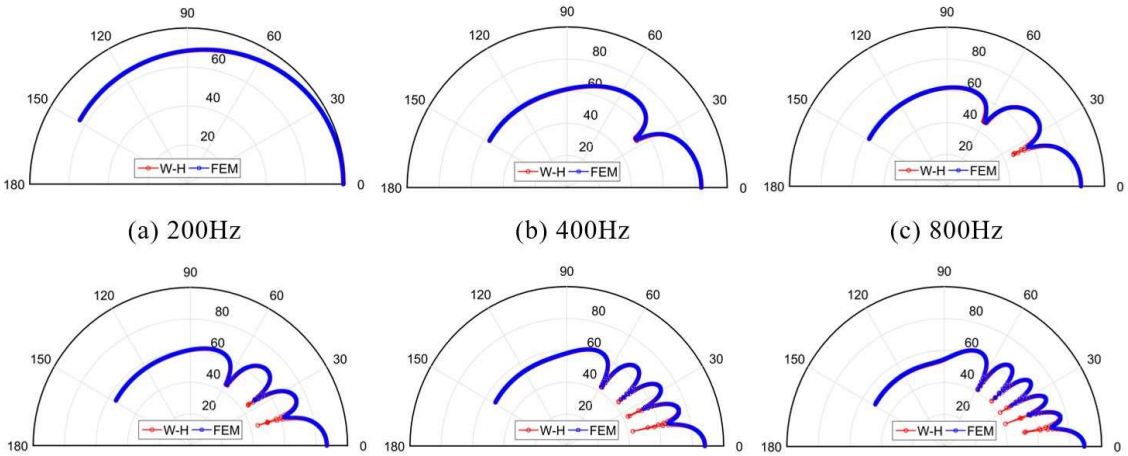

(a) 200Hz (b) 400Hz (c) 800Hz

(d) 1200Hz (e) 1600Hz (f) 2000Hz

Figure 5 – Directivity patterns of the radiated sound fields (Sound pressure level/dB) obtained by the Wiener-Hopf technique and the FEM at different frequencies (r=5m)

We also calculate the sound fields of lager enclosures at higher frequency range, the results from the Wiener-Hopf technique and the FEM coincide well with each other (The results are not listed for the limitation of pages). As the increase of geometry size and frequency, the calculation time remains nearly the same for the proposed method as it is an analytical solution. Despite the fact that, the mode number in the calculation will increase for larger size enclosure and high frequency so as to capture high order mode. The calculation efficiency is still high using the Wiener-Hopf technique because it is

easy for computer to do mode superposition. However, the meshes for the FEM increase exponentially which results in the low efficiency. So, in this condition, the Winer-Hopf technique performs much better than the FEM.

4. CONCLUSIONS

In this paper, a rigorous and explicit solution is obtained for the prediction of sound fields inside and outside a semi-infinite long enclosure. In the proposed method, the unbaffled opening of the enclosure and the ground effect are taken into consideration simultaneously in order to model the practical traffic facilities. The boundary value problem is formulated as a modified Wiener-Hopf equation involving three sets of unknowns satisfying three infinite systems of linear algebraic equations which can be solved numerically. Results obtained from the FEM and the Wiener-Hopf technique are compared and discussed which indicates that the proposed method is capable of predicting the sound fields inside and outside a tunnel simultaneously and show better performance in big size condition.

ACKNOWLEDGEMENTS

The authors would like to acknowledge the funding support from The Hong Kong Polytechnic University (PolyU152029/17E) and (PolyU152666/16E). The first author would also like to thank the studentship of The Hong Kong Polytechnic University.

REFERENCES

1. Li KM, Iu KK. Propagation of sound in long enclosures. The Journal of the Acoustical Society of America. 2004 Nov; 116(5):2759-70.
2. Law MK, Li KM, Leung CW. Noise reduction in tunnels by hard rough surfaces. The Journal of the Acoustical Society of America. 2008 Aug; 124(2):961-72.
3. Heutschi K, Bayer R. Sound radiation from railway tunnel openings. Acta Acustica United with Acustica. 2006 Jul 1; 92(4):567-73.
4. McAlpine A, Daymond-King AP, Kempton AJ. Sound radiation from a flanged inclined duct. The Journal of the Acoustical Society of America. 2012 Dec; 132(6):3637-46.
5. Research Committee of Road Traffic Noise in Acoustical Society of Japan. ASJ prediction model 1998 for road traffic noise. J. Acoust. Soc. Jpn.. 1999; 55(4):281-324.
6. Maekawa Z. Noise reduction by screens. Applied acoustics. 1968 Jul 1; 1(3):157-73.
7. Duan W, Kirby R. A hybrid finite element approach to modeling sound radiation from circular and rectangular ducts. The Journal of the Acoustical Society of America. 2012 May; 131(5):3638-49.
8. Félix S, Doc JB, Boucher MA. Modeling of the multimodal radiation from an open-ended waveguide. The Journal of the Acoustical Society of America. 2018 Jun 13; 143(6):3520-8.
9. Levine H, Schwinger J. On the radiation of sound from an unflanged circular pipe. Physical review. 1948 Feb 15; 73(4):383.
10. Gabard G, Astley RJ. Theoretical model for sound radiation from annular jet pipes: far-and near-field solutions. Journal of Fluid Mechanics. 2006 Feb; 549:315-41.
11. Rawlins AD. The solution of a mixed boundary value problem in the theory of diffraction by a semi-infinite plane. Proceedings of the Royal Society of London. A. Mathematical and Physical Sciences. 1975 Nov 25; 346(1647):469-84.
12. Mittra R. Analytical techniques in the theory of guided waves. Macmillan Series in Electrical Science. 1971.